

X- and Gamma-Ray Flashes from Type Ia Supernovae?

Peter Höflich¹ and Bradley E. Schaefer²

ABSTRACT

We investigate two potential mechanisms that will produce X-ray and γ -ray flashes from Type Ia supernovae (SN-Ia). The first mechanism is the breakout of the thermonuclear burning front as it reaches the surface of the white dwarf. The second mechanism is the interaction of the rapidly expanding envelope with material within an accretion disk in the progenitor system. Our study is based on the delayed detonation scenario because this can account for the majority of light curves, spectra, and statistical properties of 'Branch-normal' SN-Ia. Based on detailed radiation-hydro calculation which include nuclear networks, we find that both mechanisms produce brief flashes of high energy radiation with peak luminosities of $10^{48} - 10^{50}$ erg/sec. The breakout from the white dwarf surface produces flashes with a rapid exponential decay by 3 to 4 orders of magnitude on time scales of a few tenths of a second and with most of the radiation in the X-ray and soft- γ -ray range. The shocks produced in gases in and around the binary will produce flashes with a characteristic duration of a few seconds with most of the radiation coming out as X and γ -rays. In both mechanisms, we expect a fast rise and slow decline and, after the peak, an evolution from hard to softer radiation due to adiabatic expansion. In many cases, flashes from both mechanisms will be superposed. The X- and γ -ray visibility of a SN-Ia will depend strongly on self absorption within the progenitor system, specifically on the properties of the accretion disk and its orientation towards the observer. Such X-ray and γ -ray flashes could be detected as triggered events by Gamma-Ray Burst (GRB) detectors on satellites, with events in current GRB catalogs. We have searched through the GRB catalogs (for the BATSE, HETE, and Swift experiments) for GRBs that occur at the extrapolated time of explosion and in the correct direction for known Type Ia supernovae with radial velocity of less than $3,000 \text{ km s}^{-1}$. For BATSE about 12.9 ± 3.6 nearby SNe Ia should have been detected, but only 0.8 ± 0.7 non-coincidental matches have been found. With the HETE and Swift satellites, we expect to see 5.6 ± 1.3 SN-Ia flashes from

¹Dept. of Physics, Florida State University, 315 Keen Building, Tallahassee, Florida, 32306-4350

²Department of Physics and Astronomy, Louisiana State University, Baton Rouge, Louisiana 70803

known nearby SNe Ia but, yet, no SN-Ia flashes were detected. With the trigger thresholds for these experiments and the upper limits on the SN-Ia distances, we show that the bolometric peak luminosity of SN-Ia Flashes must be less $\sim 10^{46}$ erg s⁻¹. Our observational limit is several orders-of-magnitude smaller than the peak luminosities predicted for both the early flash. We attribute this difference to the absorption of the X- and γ -rays by the accretion disk of large scale height or common envelope that would be smothering the white dwarf.

Subject headings: supernovae: general - shock waves - gamma rays: bursts

1. Introduction

The history of Gamma-Ray Bursts (GRBs) started out with a supernova (SN, SNe plural) connection when Stirling Colgate calculated that the shock breakout of a Type II SN should create a burst of gamma radiation (Colgate 1968; 1970; 1974), and then he asked the Los Alamos Vela group to see if they could recognize such events. Indeed, Klebesadel, Strong, & Olson (1973) discovered the Gamma-Ray Burst phenomenon, although it was quickly realized that the shock breakout from Type II SN would not occur at gamma ray photon energies.

GRBs must necessarily pack large amounts of energy in a small volume, so attempts to link GRBs and SNe have persisted since 1973. From 1979 until the 1990's, a strong link (Felton 1982) was provided by the unique and bright burst seen on 5 March 1979 (Cline et al. 1980) coming from near the middle of a supernova remnant in the Large Magellanic Cloud (Evans et al. 1980). However, we now realize that this event is a separate subclass of bursts, called the Soft Gamma Repeaters, that apparently are magnetars and completely separate from the classical GRBs (Hurley 2000).

The first strong SN/GRB connection was made when the burst GRB 980425 was found to have a coincidence in time and position to SN 1998bw (Galama et al. 1998). The GRB was lower in luminosity than other known GRBs by many orders of magnitude and the SN was a highly unusual Type Ic SN with very high expansion velocities and a record breaking radio luminosity (Kulkarni et al. 1998). So both GRB and SN were so unusual that it was risky to generalize the connection to all events. Over the next few years, various late-time bumps in the light curves of burst afterglows have been claimed to be an underlying supernova (Bloom et al. 1999; Reichart et al. 1999; Galama et al. 2000), but these claims all had poor data and bumps are seen in afterglow light curves on all time scales so there is no reason to connect any particular bumps with supernovae. A stronger SN/GRB connection was made

with the discovery of high-velocity high-excitation absorption lines in the spectrum of GRB 021004 points to the GRB progenitor being a Wolf-Rayet star (Schaefer et al. 2003). Various groups also sought statistical connections between SNe and GRBs. The first claim (Wang & Wheeler 1998) was that bright and well-observed Type Ib/c SNe are statistically correlated with GRBs. This connection has been strongly rejected on statistical grounds (Deng 2001; Schaefer & Deng 2000) as well as through the use of better GRB error boxes (Kippen et al. 1998). Soon, claims had been made connecting specific Type IIIn SNe with GRBs (Terlevich & Fabian 1999), but these also have low significance (Deng 2001; Schaefer & Deng 2000). In the meantime, strong theoretical models were being developed which connect long-duration GRBs with the core collapse of very massive stars with fast rotation (MacFadyen, Woosley, & Heger 2001; Woosley & Bloom 2006). In 2003, the HETE2 satellite discovered a relatively nearby normal burst (GRB 030329) which displayed an afterglow spectrum like SN 1998bw starting in the week after the burst (Stanek et al. 2003; Hjorth et al. 2003). Further high-confidence associations between normal GRBs and Type Ic SNe have been made for GRB 031203 and SN 2003lw (Malesani et al. 2004) and for GRB 060218 and SN 2006aj (Campana et al. 2006). With all these strong and weak connections, the community is now confident that almost all the long-duration GRBs are associated with a core collapse supernova explosion.

This still leaves open the question of whether the short duration GRBs (Cline & Desai 1974; Kouveliotou et al. 1993) are associated with SNe? The currently popular model is that the short GRBs are caused by the collision of two neutron stars in a binary orbit which in-spirals due to gravitational wave emission (Taylor 1994). Many reasonable alternatives have been proposed (Dado & Dar 2005), including carbon-oxygen white dwarf and neutron star mergers (Dar & DeRujula 2004), gravitational collapse of a neutron star to form a quark star (Dar 1999), super-flares from Soft Gamma Repeaters in nearby galaxies (Hurley et al. 2005), or just simply some variation on the long-duration GRB core collapse. A substantial advance was made with the identification of five x-ray and three optical afterglows associated with short duration bursts (Gehrels et al. 2005; Villasenor et al. 2005; Burrows et al. 2005; Fox et al. 2005; Hjorth et al. 2005; Soderberg et al. 2006). These afterglows are associated with moderately bright and nearby galaxies, but this must be some sort of selection effect as many other short bursts certainly have no galaxy association to deep limits (Schaefer 2006). The three afterglows with optical positions are associated with the outer parts of the galaxies and with elliptical galaxies; both of which strongly point to the progenitors being in an older population. In addition, very strong limits have been placed to show that there are no supernovae associated with the bursts (Fox et al. 2005; Hjorth et al. 2005; Berger et al. 2005; Bloom et al. 2006). In all, it does appear that the short duration GRBs are an old population, often do not have an associated supernova, and are a separate population from

the long duration GRBs.

The purpose of this paper is to examine another connection between GRBs and SNe. In particular, we calculate that Type Ia SNe should produce short duration flashes of X-rays and γ -rays that would appear as short duration GRBs and would be discovered with past and current GRB detectors. It is possible that relatively nearby SN-Ia events will produce an X-ray or γ -ray flash that is bright enough to be detected. It may be worth mentioning that x/gamma-ray flashes from a GRB-connected SN (i.e. SN2006aj) might have already been detected in GRB060218, as suggested by Campana et al. (2006) and Waxman et al. (2007). Such flashes might either be labeled as short duration GRBs or as X-Ray Flashes (Heise et al. 2001; Kippen et al. 2001). We do not think that the flashes from SN-Ia events can account for the diversity of either the short duration GRBs or the X-Ray Flashes, so we are expecting that the SN-Ia flashes are only a subset of the triggered events.

Our original motivation for this study was the realization that the inevitable shock breakout of a Type Ia event will likely produce a burst of X- and γ -radiation lasting for perhaps seconds of time. The mechanism is similar to that of the original Colgate proposal for Type II SNe, however, with the distinguishing feature that, initially, the front starts as a weak detonation which is propelled by nuclear burning with time scales of seconds, and on an already rapidly expanding background. The result of the nuclear burning front should be a heating of the outermost material to a temperature of tens of keV that will last for a few seconds until adiabatic cooling (from the expansion of the material and balanced by nuclear burning) reduces the temperature. During this brief time interval, the emission will be of hard radiation from a surface area with a characteristic radius of $\approx 10^{10}$ cm. Such a source would produce a short burst of X and gamma radiation which should be visible over gigaparsec distances. To retain a distinction with the GRB phenomenon, we will label these events as 'SN-Ia Flashes'.

2. Radiation Hydrodynamical Models for Thermonuclear Supernovae

The basic explosion mechanism for Type Ia Supernovae is that carbon burning in the center of a white dwarf (WD) leads to a thermonuclear runaway because the degenerate electron gas shows hardly any temperature dependence, and the energy release results in the explosion. To first order, the outcome hardly depends on details or even the general scenario because nuclear physics determines the structure of the WD and the energy release, which causes 'stellar amnesia' (Höfllich et. al 2003). The apparent homogeneity of SN-Ia events does not imply an unique explosion scenario but masks the complexity of a phenomenon which includes stellar evolution, rotation and mass loss, accretion physics, physics of the

ignition process, propagation of nuclear flames and transport phenomena.

Within this general picture, two classes of models are most likely realized: (1) An explosion of a carbon/oxygen WD with a mass close to the Chandrasekhar limit (M_{Ch}), which accretes matter through Roche-lobe overflow from an evolved companion star (Whelan & Iben, 1973). In this case, the explosion is triggered by compressional heating near the WD center. Alternatively, (2) the SN could be an explosion of a rotating configuration formed from the merging of two low-mass WDs, after the loss of angular momentum due to gravitational radiation allows for collapse (Webbink 1994, Paczyński 1985, Benz et al. 1990).

The last decade has witnessed an explosive growth of high-quality data which allow study of second order effects. In combination with advances in computational methods, this provided new insights into the physics and a link to observations. The majority of SN-Ia seems to originate from the explosion of a WD close to M_{Ch} (Höflich & Khokhlov 1996). Based on detailed analyses of light curves and spectra, the most likely scenario involves an early phase of deflagration burning which is followed by a phase of detonation (DDT, see below), called delayed detonation models (Khokhlov 1991). An initial deflagration phase is needed for M_{Ch} mass WDs to allow for the production of intermediate mass elements, and a subsequent detonation phase is required to be in agreement with the overall radially layered chemical structure and the observation that almost the entire WD is burned. For recent reviews, see Branch (1999), Höflich (2006), and Nomoto (2003).

Here, we want to mention two results directly relevant for bursts, and which set the tone. In a recent study of early time spectra of several SN-Ia, Quimby et al. (2005) established that, as suspected (e.g., Branch 1999, Höflich 1995, Marion et al. 2003), the nuclear burning front reaches the very outer layers of SN-Ia where the outer layers of SN expand with velocities in excess of 25,000 km/sec. Secondly, high velocity Ca II has been found to be a common feature in SN-Ia (Fisher et al. 1999, Wang et al. 2003). Gerardy et al. (2004) studied the formation of the high velocity Ca II feature and its diagnostics based on detailed NLTE-models. They showed that this feature and its evolution with time can be understood in the framework of the interaction of the ejecta with a circumstellar shells of solar composition which, likely, has been part of the progenitor system/accretion disk with a dimension of $2 - 10 \times 10^{10}$ cm (Iben & Tutukov 1975). Interaction with a wind was excluded because ongoing interaction would dominate the luminosity of SNe Ia. Quimby et al. (2005) applied this diagnostics to several supernovae and estimated the mass of the shell to be between 10^{-3} to $2 \times 10^{-2} M_{\odot}$. These estimates are consistent with the upper limits based on hydrogen emission by Cunnig et al. (1989) and, more recently, Mattila et al.(2005).

Our study is based on the delayed-detonation scenario because it reproduces the optical and infrared light-curves and spectra and the statistical properties of typical SN-Ia reasonably

well. During the early phase, the flame propagates as a deflagration, i.e. the unburned matter is ignited by heat conduction over a front propagating with an effective velocity of a few percent of the speed of sound. After burning $\approx 0.3M_{\odot}$ of the carbon/oxygen WD, the detonation is triggered. In a detonation, the matter is ignited by compression and the front is driven by nuclear burning behind the front.

We consider two possible origins for X-ray and γ -ray flashes. The first possibility is the breakout of the (nuclear) burning front on the surface of the white dwarf, and the second possibility is the interaction of the rapidly expanding envelope with material in an accretion disk within the progenitor system. In either case, the high energy ultimately comes from the thermonuclear energy. The total amount of energy available is determined by the thermal and total energy content of the outer layers in case of the outbreak and interaction, respectively.

2.1. Numerical Methods and Setup

The computations have been performed using our HYDrodynamical RAdation code (HYDRA) which is based on modules used to carry out many prior studies of SN-Ia. Previous applications include detailed, hydrodynamical calculations including detailed nuclear networks, γ -ray transport in spherical and 3-D geometry, and detailed NLTE light curves and spectra (Höfllich 1988, Höfllich, Müller & Khokhlov 1993, Höfllich 1995, Howell et al. 2001). For technical details of HYDRA, see Höfllich et al. (1998), Höfllich (2002ab), and references therein.

Parameters were chosen, which roughly match the observed properties of normal Type Ia supernovae. We consider the explosion of a Chandrasekhar mass white dwarf which originates from a star with a main sequence mass of $5 M_{\odot}$ and solar composition. At the time of the explosion, the central density is $2 \times 10^9 \text{ g cm}^{-3}$. The nuclear burning starts as a deflagration with a parameterized description of rate of burning based on 3-D models by Khokhlov (2001). When the density reaches $\rho_{tr} = 2.5 \times 10^7 \text{ g cm}^{-3}$, the detonation is triggered. Although we consider a specific model, the results are more generally applicable since the structure of the WD, the explosion energy, and the light-curves are mainly determined by nuclear physics rather than the details of the nuclear burning (“stellar amnesia”; Höfllich et al. 2003). From the setup, the model is identical to 5p0z22.25 of Höfllich et al. (2002) but with some technical modifications to allow for this study. The explosion is calculated for the first 30 seconds including simultaneously the hydrodynamics, the nuclear reaction networks with 218 isotopes, radiation transport modules that take into account relativistic corrections (Mihalas, Kunacz & Hummer 1976), and the time dependence for the radiation transport. We consider 800 frequency groups ranging from 10^{-5} to 3 MeV . For the opacities, we include bound-

free, free-free and Compton scattering, pair production and inverse reactions, and nuclear reactions (Höfllich 1991, Höfllich 2005). We assume full ionization rather than detailed atomic models because temperatures are of the order of $10^7 - 10^9$ K. Our hydrodynamics code uses a fixed grid with a mass resolution of $2 \times 10^{-6} M_{\odot}$ in the outer layers of the WD. For the radiation transport, we allow for 7 levels of rezoning to increase the effective resolution by up to a factor of 2^7 , i.e. to $2 \times 10^{-8} M_{\odot}$. Hydrodynamical quantities are interpolated using ‘rotated parabolae’.

2.1.1. *The Evolution and the Shock Breakout*

In Fig. 1, we show the structure of the exploding WD during several phases. During the subsonic deflagration phase (a), the nuclear energy release causes a pre-expansion of the entire WD from about 1700 km to ≈ 5500 km. Burning in the inner layers pushes the outer layers. Most of the nuclear energy is used to lift the WD in its gravitational potential and even at the outer layers, the expansion velocity remain less than a few thousand km/sec even at the outermost layers. During this phase, the temperature of the burned matter reaches well in excess of 5×10^9 K behind the front, and adiabatic cooling causes the temperature to drop in the unburned region. Subsequently, a weak detonation front (b) travels through the expanding WD at velocity slightly larger than sound speed and heats the WD to temperatures of a few times 10^9 K. Nuclear burning behind the front drives the compressional wave and causes the expansion of the matter behind the front at an accelerated rate. At about 2.3 seconds, the detonation front reaches the surface and heats the outermost layers to $\approx 1.5 \times 10^9$ K. Over the following few tenths of a second, these layers are accelerated up to about 80,000 km/sec. The further evolution is governed by adiabatic expansion, modified by ongoing nuclear burning and radiative cooling at the outermost layers. After about 5 to 10 seconds, the expansion is almost homologous, i.e. the velocity is proportional to the distance. Expansion velocities exceed 30,000, 40,000 and 80,000 km/sec at the outermost 10^{-2} , 10^{-4} , and $10^{-5} M_{\odot}$, respectively.

The nuclear burning time scales increase with decreasing density. As a consequence, only incomplete burning takes place throughout the outer half of the WD (in mass). This property is well established by observations which show incomplete Si burning as well as explosive oxygen and carbon burning. Almost the entire WD undergoes burning with exception of the outermost $10^{-4} M_{\odot}$ (Fig. 2). However, the shock front does not stop its propagation and it still heats the surface layer. In this context, we want to mention one of the major uncertainties related to the shock breakout. The initial WD grows by accretion of H or He-rich matter. As a result, we can expect He (and H)-rich surface layers in the outer few

times $10^{-6}M_{\odot}$. Helium burns on significantly shorter time scales compared to carbon and can produce additional nuclear energy even under low density conditions. The details depend sensitively on the amount of unburned H/He, mixing processes between the H/He and the C/O layers. Test calculations showed variations in peak luminosity during the outbreak by a factor of ~ 3 from the specific model considered here.

2.2. The Shock Breakout

The mechanism of the X- and gamma-ray production is similar to the Colgate mechanism in core collapse supernovae where a shock steepens, however, with several distinguishing features. In core-collapse SNe, the temperature increases by a strong detonation front whereas, in thermonuclear supernovae and, within the now widely accepted delayed detonation scenario, the front propagates even close to the surface as a weak detonation driven by ongoing thermonuclear reactions which bring up the temperatures to billion degrees, and this front steepens close to the surface. The e^+ , e^- pairs will be formed in the dense matter of the expanding envelope and annihilate almost instantly so the compactness problem could be avoided and the high energy photons can escape the system. Most of the hard radiation is emitted when the energy is released from dense matter when it becomes transparent due to expansion.

As mentioned above, the outermost region is heated by the propagating shock front to a peak temperature of $\approx 1.5 \times 10^9$ K. The luminosity is governed by the decrease of the optical depth due to geometrical dilution, adiabatic cooling and, somewhat, energy production by ongoing nuclear burning.

The time scale for the burst luminosity is set by the rate of expansion and run time effects (Fig. 3). At the time of the outbreak, the radius of the object is about 9000 km, and thermalization is almost instantaneous. As a result, the luminosity of the pre-expanded WD rises within about 1/30 of a second starting from a luminosity of about 10^{38} erg. Subsequently, the matter undergoes rapid acceleration from $\approx 10,000$ km/sec to 80,000 km/sec on time scales of a 0.2 to 0.3 seconds during which the radius increases by a factor of 7. The result is a flash light curve with a fast rise and a slower decline which reaches a peak luminosity of $\approx 5 \times 10^{49}$ erg/sec for a few hundredths of a second with an extended tail.

The observable shock breakout is not thermal because multiple scattering by thermal electrons (Pozdnyakov et al. 1976), the frequency dependence of the opacity and, thus, different layers contribute to the spectrum, and run time effects due to the extension of the source, i.e. the evolution over the expansion times. We have added a corresponding note in

section 2.2

The monochromatic light curves show a low energy precursor in the 0.1 keV range, early hard radiation up to the MeV range followed by a rapid shift to hard X-rays on time scales of 0.1 to 0.3 seconds. And a softening of the X-ray spectrum over 5 to 10 seconds. Note that the decreasing Compton opacity with wavelength and multiple scattering is crucial for hardening the radiation, an effect that is well known from hot stars.

2.3. Interaction within the Progenitor System

Up to now, we have considered the exploding WD in 'isolation' neglecting the secondary X-rays and γ -rays in context of thermonuclear explosions. As discussed above, the WD is member of a close binary system with an accretion disk. Likely, we have seen evidence for the interaction of the expanding envelope with its surroundings. Potentially, this is a dominant contributor to the X-rays and, in particular, hard γ -rays because we can directly tap into the kinetic energy of the outer layers rather than the thermal reservoir. The available thermal energy is limited by the nuclear energy production per nucleon ($\leq 3 - 6$ MeV), whereas the available kinetic energy of the outermost matter has gained kinetic energy originating from non-local burning. As a result, mean energies per atom are in excess of 100 MeV and about 8 % (i.e., 10^{50} erg) of the total explosion energy are deposited in the outer $10^{-2}M_{\odot}$ (Fig. 2).

We have evidence for this interaction that suggests that we can tap into the energy reservoir of the outer $10^{-3} - 10^{-2}M_{\odot}$ and this is a common phenomenon. However, we have little information about the distribution and density of the surrounding matter which is critical for self-absorption, and the mechanism of transformation. Is the process dominated by bremsstrahlung, thermalization, another process (e.g. magneto-hydrodynamical effects), or a combination of all? From the specific energy of the particles in the ejecta and a H/He-rich surrounding, we may expect hard radiation somewhere between X-ray energies up to a few hundred keV.

Despite the uncertainties, we can estimate some of the properties along the lines of Sect. 2. The total dimension of the progenitor systems are of order 10^{11} cm and the accretion disk has an inner edge close to the exploding WD. As a consequence, we can expect a rapid rise of the luminosity within a fraction of a second. Taking the expansion velocities from Fig. 2, the interaction will last less than a few seconds. Thereafter, the matter is swept up and will undergo adiabatic cooling. As above, we must expect fast rise and slow decline light curves but on a longer time scale of several seconds with a comparable or slightly higher peak luminosity as compared to the shock breakout luminosity. Note that self absorption

may severely reduce the observed fluxes or may somewhat increase the time scales because of intermittent trapping of energy. Because the observability depends sensitively on the geometry of the circumstellar matter and the orientation with respect to the observer, we must expect large individual variations.

3. Correlating SNe Ia and GRBs

The goal of this section is to try to test the theoretical predictions that SN-Ia can give flashes of γ -rays that can trigger GRB detectors and look like GRBs with 1-10 second durations and fast-rise exponential-decay (FRED) light curves. In particular, we will seek to find these SN-Ia Flashes by looking for correlations between catalogued Type Ia SNe and catalogued GRBs. The result can then be used to place limits on the luminosity of SN-Ia Flashes.

The procedure is to compile a list of all known SN-Ia events (with an upper limit on their distance), estimate their date of core collapse, and seek a cataloged GRB with a consistent date and position on the sky. The reason to go in this direction is that we know the SN-Ia collapse occurred at a specific time and direction, so we have the simple question of asking whether any associated SN-Ia Flash was detected by a satellite GRB detector. In general, we cannot know the exact time of the collapse, so we cannot know whether any particular GRB detector was pointed in the right direction at the right time. This makes our test a statistical one. We can know the number of SN-Ia events that might have been covered by GRB experiments, and we can calculate what fraction of the known SN-Ia events are likely to have good coverage, so we can estimate how many of these known SN-Ia events should appear in GRB catalogs if the SN-Ia Flashes are brighter than the detection limit. If many Flashes are expected but none are detected, then we will have a limit on the Flash brightnesses. When combined with the upper limit on the distances, this will translate into an upper limit on the Flash luminosity. And this can then be compared with our earlier theoretical predictions.

This study is possible only because SN-Ia Flashes have properties similar to GRBs. In particular, SN-Ia Flashes have typical peak temperatures corresponding to 100 keV which cools substantially throughout the event, and light curves with fast rises and roughly exponential declines with time scales of a few seconds. This description of a SN-Ia Flash is identical to those of the multitude of FRED bursts. If a SN-Ia Flash is bright enough, then it would be 'hiding' inside the GRB catalog as an apparently ordinary FRED burst.

The FRED shape is a common light curve shape for individual pulses within a burst.

Yet bursts with multiple FRED pulses cannot be a SN-Ia Flash since only one white dwarf can collapse to make only one FRED. We do not know how much fluctuations to expect from turbulence in the outer layer of a WD or any surrounding gas, so the basic FRED shape can well have superposed spikes or modulations of perhaps large amplitude. A perusal of the light curves displayed in the first BATSE catalog (Fishman et al. 1994) shows that roughly 50% of all BATSE triggers are single FREDs (perhaps with significant fluctuations around the basic FRED shape) with time scales from 1-10 seconds.

3.1. GRBs Included

For this study, we will use GRBs from three satellite experiments; BATSE on the *Compton Gamma-Ray Observatory*, HETE, and Swift.

3.1.1. BATSE Bursts

The BATSE detectors covered the entire visible sky for 9.1 years, and this provides a large coverage with deep limits. We have adopted the BATSE 4B burst catalog (Paciesas et al. 1999) as well as its extensions up until the date of the satellite re-entry (BATSE GRB Team 2001). This covers 2702 triggered GRBs from 19 April 1991 until 26 May 2000 (an interval of 3323 days). This is an average of 0.813 triggered bursts per day. After accounting for Earth-blockage, SAA passages, and other inefficiencies, BATSE covered the entire sky for this time interval with an average efficiency of 39% (Fishman et al. 1994; Paciasas et al. 1999).

When we seek positional coincidences between precisely-known SN positions and the BATSE positions, we must estimate the uncertainties in the BATSE positions to know whether the positions are coincident. We will adopt the two-sigma positional error radius as a reasonable compromise between missing true connections by making the radius too small and adding false connections by making the radius too large. (Repeated calculations with 1.0 and 3.0 sigma radii yield the same results as below except with larger uncertainties.) The cataloged one-sigma radius for each individual burst is for the statistical error only, and must be increased by the systematic error of 2.0 degrees (Briggs et al. 1999) added in quadrature so as to get the total radius of the one-sigma positional error circle (σ_{BATSE}). The two-sigma radius is just twice the one-sigma radius. For the purposes of this paper, the error regions will be assumed to be circular in shape, even though individual bursts will have moderate distortions from this ideal.

The sum of the areas for the two-sigma error regions over all 2702 bursts is a total of 1.16 million square degrees. The average burst area is 431 square degrees, which is 1.05% of the sky.

The BATSE catalogs are ideal for estimating the number of bursts with a peak flux brighter than some stated threshold. For example, the cumulative distribution of bursts brighter than some give peak flux in the 50-300 keV energy band over a one second interval is given in Figure 6c of Paciesas et al. (1999). To convert this number to a rate (with units of bursts per year) for the whole sky with perfect efficiency, we have to divide by the efficiency (39%) and divide by the number of years in the 4B catalog (5.37 years). So, for a peak flux of $1.0 \text{ photons cm}^{-2} \text{ s}^{-1}$ or brighter, there are 400 BATSE bursts in the 4B catalog, and this gives a total count of 190 bursts per year appearing over the entire sky. flux of $0.5 \text{ photons cm}^{-2} \text{ s}^{-1}$, there are 700 bursts in the 4B catalog, which translates into 330 bursts per year over the entire sky.

3.1.2. HETE Bursts

HETE has detected many GRBs from roughly 2001 to 2005, while providing fast information to the ground so as to allow rapid follow-up of burst positions. We will use a catalog of 69 HETE bursts with accurate positions detected in the 4.0 year interval from 2001.0 to 2005.0 (HETE Team 2006; see also Greiner 2006).

Most HETE bursts have received substantial ground-based follow-up optical imaging in the hours and days after the burst. Greiner (2006) presents an extensive compilation of reports from this vast program. This follow-up work would likely have discovered any nearby SN-Ia event at the position of the GRB. Thus, there is no real expectation that a comparison of nearby SN-Ia lists will turn up any GRB/SN connections. As such, we are merely trying to place limits on the brightness and luminosity of any SN-Ia flashes that arise from known Type Ia supernovae.

The HETE bursts all have arc-minute positions, while the supernovae will all have arc-second positions. Should any HETE position contain any SN position, we can be confident that the positional overlap is not due to any random coincidence, and thus we would conclude that the GRB and SN are causally related. So, unlike for BATSE, we don't have to worry about false alarms due to coincidences. Rather, the primary question will be with whether HETE was actually looking at the SN position at the time of the shock breakout.

Sakamoto et al. (2005) present a compilation of the peak fluxes for many HETE bursts. We have used the peak fluxes from 30-400 keV over one-second time intervals to construct

a brightness distribution. This distribution should be rising as a power law to low peak fluxes yet with a break due to the HETE threshold. In the observed distribution, we see that the 1-3 photons $\text{cm}^{-2} \text{s}^{-1}$ bin already is substantially lower than expected from the numbers in the 3-9 photons $\text{cm}^{-2} \text{s}^{-1}$ bin, hence suggesting a break at around 2 photons $\text{cm}^{-2} \text{s}^{-1}$. But HETE detected many bursts going to peak fluxes of 0.1 photons $\text{cm}^{-2} \text{s}^{-1}$ and fainter. This broad threshold will have a 50% detection probability around 1 photons $\text{cm}^{-2} \text{s}^{-1}$. This detection threshold corresponds to roughly $1.7 \times 10^{-7} \text{ erg cm}^{-2} \text{ s}^{-1}$. From the previously stated BATSE result, this limit corresponds to 190 GRBs per year over the whole sky. As the HETE catalog reports on 69 bursts per 4.0 years, the overall fractional sky coverage by HETE must be roughly 9%. That is, any particular SN-Ia from 2001 to 2005 will have an average chance of 9% that HETE was looking at its Flash. The uncertainty on this fraction will primarily be in the systematics of the comparison between the satellites, which we estimate to be $\pm 3\%$.

3.1.3. *Swift Bursts*

Swift (Gehrels et al. 2004) was launched in late 2004 and is still recording bursts at a fast rate. We will use the Swift catalog for the 1.75 year interval from 2005.0 to 2006.75 (Swift Team 2006; see also Greiner 2006). This interval has 140 Swift GRBs with accurate position and comprehensive optical follow-up imaging. As with HETE, any nearby SN-Ia associated with the event would almost certainly have been quickly recognized (so we are not expecting to find any such connections) and the Swift positions are arc-minute in size (so there is no real chance of random coincidence producing a false alarm).

The Swift burst detector has a half-coded field of view of 1.4 steradians (Gehrels et al. 2004), which is 11% of the sky. In practice, roughly 40% of the detected Swift GRBs are with less than half-coding, so the effective coverage of the sky is 19%. The operations of the spacecraft keep the field of view of the burst detector outside of Earth occultation. With down-time largely being the small fraction due to the SAA, we estimate that the Swift sky coverage is roughly 18%. We estimate the uncertainty in this fraction to be $\pm 6\%$.

The Swift web page tabulates the peak fluxes from 15-150 keV over one-second time intervals. We have constructed a brightness distribution for these bursts. We see a fairly sharp threshold, with the 1-3 photons $\text{cm}^{-2} \text{s}^{-1}$ bin having the numbers expected (based on a power law extrapolated from the numbers in the brighter bins), while the 0.3-1 photons $\text{cm}^{-2} \text{s}^{-1}$ bin is down by almost a factor of four. On this basis, we take the Swift threshold to be close to 0.7 photons $\text{cm}^{-2} \text{s}^{-1}$. This threshold is for a passband of 15-150 keV, and this is equivalent to a threshold of roughly 0.5 photons $\text{cm}^{-2} \text{s}^{-1}$ for a pass band of 50-300

keV. From BATSE, we expect that there should be 330 bursts per year over the whole sky to this threshold. With Swift seeing 140 bursts per 1.75 years, this implies a fractional sky coverage of 24%.

3.2. Supernovae Included

For this study, we have adopted the Asiago Supernova Catalog (Barbon et al. 1999), which can be obtained as an up-to-date version on-line. From this catalog, we have extracted supernovae that are explicitly identified as being of Type Ia with dates of explosions between the start and stop dates for each of our GRB data sets. We will primarily be looking at those SNe whose host galaxy has a radial velocity (RV) of 3000 km s^{-1} or less (corresponding to a distance of 43 Mpc for a Hubble constant of $70 \text{ km s}^{-1} \text{ Mpc}^{-1}$). The reason for this cut is since we expect the SN-Ia Flashes to be primarily visible from the nearest SNe, while the inclusion of more distant events will only dilute the statistics. We have tried varying this RV cutoff, yet we reach the same conclusions.

3.2.1. For the BATSE catalog

The BATSE catalog covers from 19 April 1991 to 26 May 2000. Our sample of Type Ia supernovae in the Asiago catalog with $RV < 3000 \text{ km s}^{-1}$ includes 38 SNe. We have chosen to eliminate 5 events (SN1991ak, SN1993Z, SN1993af, SN1994aa, and SN1998cn) from this sample based on a criterion that the day of explosion must have an uncertainty of 10 days or better. (Again, the relaxation of this criterion does not change our results.) Thus, our primary sample of nearby Type Ia SNe contains 33 events (see Table 1).

For each supernova on this list, we determined the date of peak brightness (T_{peak}) from the literature. These dates are presented in Table 1. Each date also has an estimated one-sigma uncertainty. Some of these uncertainties are from formal fits of the light curve to templates, and these are assigned an uncertainty of ± 2 days. However, if a formal template fit was made to data starting after five days of the claimed maximum light, then the derived date is assigned an uncertainty of ± 5 days. The ‘snapshot’ method of Riess et al. (1998) is regarded as having an uncertainty of ± 7 days. If a peak date is assigned based on a spectrum being ‘near maximum’, then an uncertainty of ± 7 days was assigned. Other cases have uncertainties as tabulated.

For each supernova, we determined the offset between the date of the explosion and the date of the peak in the B-band. We have adopted an offset of 19.8 days for a supernova

(Riess et al. 1999b) with the stretch factor (S) equal to unity. The offset for other stretch factors is $19.8/S$ days. The measured quantity $\Delta m_{15}(B)$ is taken as $1.96(1/S - 1) + 1.07$ (Krisciunas et al. 2000). We have adopted an uncertainty of ± 2 days in the offset for SNe with a measured decline rate. If the SN does not have a measured decline rate, we adopt $S = 1$ and an uncertainty of ± 4 days for the offset. If $S < 0.75$, we take the uncertainty in the offset to be ± 4 days.

The date of the explosion (i.e., when the collapse starts the rapid brightening in the light curve) is found by subtracting the offset from the date of the peak in brightness. For each SN, we compared this with the first reported positive detection of the SN, and fortunately we had no conflicts. The result is a date of explosion (T_{exp}) for each of the 33 SNe in Table 1.

As a null test for the significance of any correlation, we have also constructed a set of dates for each SN where the offset is *added* to the date of peak. This produces a set of dates (that certainly does not include the true dates of the explosions) which have similar distributions as the real dates of explosions. The idea will be that the number of GRB/SN matches for this 'time-reversed' set should provide a measure of the false alarm rate for matches.

We have also created a sample of SN-Ia events with a radial velocity between 5,000-10,000 km s⁻¹. The events in this high RV sample typically have ~ 4 times the distance as SNe in our primary sample ($< 3,000$ km s⁻¹). Thus, any SN-Ia Flashes in the high velocity sample will be ~ 16 times fainter than in our primary sample. Provided that SN-Ia Flashes do not have a broad luminosity function, the presence of a substantial number of SN-Ia Flashes in the high velocity sample would force the presence of many and bright SN-Ia Flashes in the low velocity sample. This would be obvious, whereas the few possible matches involve faint bursts near the BATSE threshold. As such, any SN-Ia Flashes from the distances corresponding to 5,000-10,000 km s⁻¹ would have been below the BATSE threshold. One implication of this is that the high velocity sample can be used as a control sample for estimation of the number of coincidental matches in our primary sample.

3.2.2. For the HETE and Swift Catalogs

The effective dates for the HETE and Swift GRB data sets are 2001.0 to 2005.0 and 2005.0 to 2006.75 respectively. The Asiago SN catalog returns 30 and 16 SN-Ia events (with $RV < 3000$ km s⁻¹), respectively. These SNe are not separately listed because there are no SN/GRB matches.

3.3. The Observed Matches

If some (or all) Type Ia events produce an observable burst of gamma radiation (a SN-Ia Flash), then there should often be a matching burst detected by the satellites. How many of the nearby SN-Ia in the Asiago catalog have a match with a cataloged γ -ray event?

3.3.1. BATSE/SN Matches

For each of the 33 SNe in Table 1, the BATSE catalog was searched for any event that coincided in both time and direction. That is, the dates of the GRB and the SN explosion must match to within the stated error bars and the two positions must agree to within the two-sigma positional error bar. For all the matches, Table 1 lists the BATSE burst, the angular separation between SN and GRB (Θ) divided by σ_{BATSE} , and the time difference between the GRB and SN explosion (ΔT). In italics, we have also added the information for the matches where the angular separation is from 2 to 3 sigma.

We checked to see if the InterPlanetary Network (IPN; Hurley et al. 1999; 2000) could be used to reduce the size of the GRB error boxes. The idea is that smaller error boxes will either increase the confidence in the GRB/SN connection or will eliminate the possibility. Unfortunately, none of the listed bursts have IPN error boxes.

In all, for the 33 nearby Type Ia SNe during the BATSE era, four GRBs are consistent in time and within the two-sigma positional error box. If we expand the positional error boxes for the GRBs to a three-sigma cut, then we have 10 matches. If we restrict the cut to one-sigma boxes, then we have two matches.

The individual bursts with good matches are good candidates for SN-Ia Flashes. As such, the associated gamma-ray events were examined closely to see if they shared any common features. For example, we looked at the light curve shape, the duration, the smoothness of the light curve, the spectral lag of the light curve, and the BATSE hardness ratio. We could find no common traits shared by the matches. However, we found that all the matches were with faint BATSE bursts (which must necessarily have large positional error boxes). This is exactly what we would expect if the matches are random coincidences.

Two of our matches (SN1991bg/GRB911125 and SN1997bq/GRB970331) are events with a FRED light curve and time scales from 1-10 seconds. As such, these two events are particularly interesting as possible SN-Ia Flash candidates. However, roughly half of all GRBs appear as single-episode fast-rising events with a slower decline (perhaps with fluctuations) with time scales of 1-10 seconds. So the presence of two FREDs amongst our

four matches implies that the FRED shape of two matches is not significant.

As a statistical control, we also checked a group of distant SNe for matches with GRBs. In particular, we examined 66 Type Ia events with host galaxy radial velocities from 5,000 to 10,000 km/s as extracted from the Asiago catalog. We searched for matches to GRBs which occurred anytime in the month prior to the date recorded in the Asiago catalog (usually the discovery date). This set of date ranges and positions should have similar distributions as for our primary set of nearby SNe. The result was 17 matches within the two-sigma GRB error radii.

For the 'time-reversed' set of explosion times, a similar collection of matches was made. The number of matches was 1, 4, and 9 for the one-sigma, two-sigma, and three-sigma error boxes respectively.

3.3.2. *HETE/SN and Swift/SN Matches*

We examined our lists of selected SN-Ia events against the HETE and Swift GRB lists. No matches were found, with all pairs being far from acceptable. This is not surprising, as any SN that would have appeared in a GRB error box would likely have been quickly discovered and widely known by now.

3.4. The Expected Number of Coincidental BATSE/SN Matches

Our basic sample of 33 SNe has resulted in 4 matches (for two-sigma error boxes) with BATSE bursts. Some number (perhaps all) of these matches could be due to random coincidences. This section will evaluate the number of expected coincidences by three methods.

Each SN in Table 1 has a stated uncertainty for the date of the explosion. As this interval is two-sided, the time during which a GRB coincidence would be accepted is twice that amount. When summed over all 33 SNe, the total time interval is 364 days. The probability that a GRB will randomly occur with an error box that includes the SN position and at a time consistent with a specified SN is simply the average burst rate (0.813 burst/day) times the fraction of the sky that is covered by an average GRB error circle (1.05%) times the total time interval in which the explosion is constrained (364 days). Thus, the expected number of coincidental matches is 3.1 bursts.

This simple calculation will be inexact if the GRBs and SNe are clumped in time and position. Indeed, the GRBs were discovered at rates which vary with the BATSE trigger

criteria and solar activity while the SNe rates peak in the seasons when high galactic latitudes are near the meridian at midnight. Also, the SNe are strongly concentrated towards the galactic poles while the BATSE bursts are essentially isotropic. These nonuniformities will create correlations that will systematically distort the estimated number of coincidental matches by some small percentage.

The set of 'time-reversed' dates provides a sample with similar distributions in time and direction as the real sample of explosion dates. The number of matches between this time-reversed data set and the real BATSE burst catalog will share all the effects as caused by the various nonuniformities, yet none of the matches can be caused by a real SN-Ia Flash. Thus, the observed number of time-reversed matches should be equal (within the usual Poisson statistics) to the number of coincidental matches contained in Table 1. This number has already been identified as 4 matches in the time-reversed data set. The uncertainty is ± 2 bursts.

The set of SNe with radial velocities between 5,000 and 10,000 km/s has the same distribution over time and over the sky as our primary set with radial velocities of $< 3,000$ km/s. Thus, the rate of coincidental matches between this high velocity SNe sample and BATSE GRBs should be the same as for our primary low velocity sample. Out of 66 high velocity SNe, 17 had matches with the BATSE catalog. Each high velocity SNe had a time interval of one calendar month (an average of 30.4 days) for the match, with a total time interval of 2006 days. Thus, the control sample had an average of one match every 118 days. The 33 SNe in our primary sample had a total time interval of 364 days, so we would expect 3.1 matches by coincidence alone. The uncertainty in this estimate comes by propagating the Poisson noise for the original 17 count, so that the error bar will be 24%. In all, this control sample gives a rate of 3.1 ± 0.7 coincidental matches for our primary sample.

Our primary sample of 33 SNe produced 4 matches out of which some number are purely coincidental matches. We have just estimated the number of coincidental matches to be 3.1, 4 ± 2 , and 3.1 ± 0.7 . The first estimate suffers from unknown systematic errors due to the clumpiness of GRBs and SNe in time and space, so we will only use it to provide confidence that the more complex methods are not greatly in error. The remaining two estimates are independent and hence can be combined as a weighted average to yield our final value for the false alarm rate of 3.2 ± 0.7 coincidental matches. When the number of coincidental matches is subtracted from the 4 observed matches, we are left with a 0.8 ± 0.7 matches as being of non-coincidental origin. This is consistent with a null detection of SN-Ia Flashes. That is, the observed number of matches is consistent with being entirely due to random overlaps with no physical connection between the gamma ray event and the SNe. Alternatively, we can place a one-sigma upper limit on the number of SN-Ia Flashes in the BATSE data as

1.5 matches.

3.5. Limits on Luminosity and Covering Fraction

Our searches for BATSE, HETE, and Swift are all consistent with zero SN/GRB matches. For BATSE, the large error boxes and the resultant likelihood of chance coincidences only allows us to place a one-sigma upper limit of 1.5 matches. For HETE and Swift, with their small error boxes, we know that there are 0 and 0 matches respectively. Our lack of matches could be due to the detectors not happening to point at the SN-Ia at the time of collapse, the SN-Ia luminosity being too low to allow for detection, or the shock breakout being covered by some object (the companion star or the accretion disk) in the progenitor. With the above information, we can calculate how many of the nearby SN-Ia events will likely have been in the field-of-view of each of the satellites. From this, we can then place a limit on the luminosity of the SN-Ia Flashes. Alternatively, we could place limits on the covering fraction, where the companion star or the accretion disk hides the shock breakout from view here at Earth.

3.5.1. BATSE Limits

BATSE had a significant fraction of deadtime in its coverage of any one location on the sky. This fraction is 39% (e.g., Fishman et al. 1994), and represents normal blockage by the Earth, deadtime due to the South Atlantic Anomaly, and other inefficiencies. This means that out of the 33 SNe in our primary sample, only 12.9 ± 3.6 SN-Ia Flashes *could* have been detected by BATSE. The difference between 12.9 ± 3.6 and 0.8 ± 0.7 could be either due to some fraction of the SN-Ia Flashes being covered (say, by an accretion disk) that hides the flash from some directions or by the luminosity of SN-Ia Flashes being so low that many of the SN-Ia Flashes in the sample volume (out to 43 Mpc) would be below the BATSE threshold.

BATSE was operating and monitoring the sky at the times of the shock breakouts for 12.9 ± 3.6 nearby Type Ia SNe. The lack of observed GRB/SN matches (above chance coincidence) could be simply due to the SN-Ia Flashes being too faint for BATSE to detect. The BATSE trigger threshold is 3×10^{-8} erg s⁻¹ cm⁻² or 0.2 photon s⁻¹ cm⁻² for the 1.024 second trigger time scale (Fishman et al. 1994). The 12.9 nearby supernova must be at a distance closer than 43 Mpc. For them not to be detected due to low luminosity, their luminosities must all be below 7×10^{45} erg s⁻¹ (in the 50-300 keV energy band for the usual

BATSE trigger). If the average SN-Ia Flash luminosity is lower than this upper limit, then BATSE will detect events only within a smaller volume and this will reduce the expected number of matches. To reduce the expected number from 12.9 (for relatively high luminosity SN-Ia Flashes) to 1.5 (the one-sigma upper limit on the observed matches), the radius of the volume must decrease from 43 Mpc to 21 Mpc. A detection limit of 21 Mpc corresponds to a limit on the average SN-Ia Flash luminosity of 2×10^{45} erg s⁻¹ (for the 50-300 keV band). For a spectrum with a spectral peak at 100 keV, the bolometric peak flux will be 2.4 times the 50-300 keV peak flux. Thus, if the lack of observed BATSE/SN matches is caused by SN-Ia Flashes having low luminosity, then our observational limit is 5×10^{45} erg s⁻¹ for the bolometric peak flux.

The limit derived in the previous paragraph applies to the BATSE trigger time scale of 1.024 seconds, as is optimal for the flash arising from interaction with the accretion disk. But the shock breakout has a time scale of peak emission of roughly 0.1 sec, so the flux averaged over any 1.024 second interval would be smaller by a factor of ten. For these fast time scales, BATSE also has triggers that operate on 0.064 and 0.256 sec time scales. The BATSE trigger threshold is 1.5×10^{-7} erg s⁻¹ cm⁻² or 1.0 photon s⁻¹ cm⁻² for the 0.064 second trigger time scale (Fishman et al. 1994). For a detection limit of 21 Mpc, the limit on the Flash luminosity is 1×10^{46} erg s⁻¹ for the 50-300 keV band or 2×10^{46} erg s⁻¹ for the bolometric peak flux.

If some fraction, F , of the SN-Ia Flashes are uncovered and visible from afar, then the expected number of SN-Ia Flashes in our sample would be $12.9 \times F$. (This assumes that all SN-Ia Flashes are luminous enough to be detected by BATSE out to distances of 43 Mpc.) The best estimate of F is then $0.8/12.9=0.062$. However, the uncertainty in F is large. For a value of $F=0.12$, the expected number of matches will equal the one-sigma upper bound on the number of observed SN/GRB matches. Thus, the near zero number of matches might imply that $> 88\%$ of the SN-Ia Flashes are usually covered by something like an accretion disk and are hidden from view.

3.5.2. HETE Limits

HETE was up and watching the sky during the time when 30 nearby SN-Ia events occurred. Of these 30, we expect that $9\% \pm 3\%$ will have HETE pointed in the right direction at the right time. So we expect 2.7 ± 0.9 SN-Ia Flashes that HETE could have detected. But HETE saw 0 matches. For a Poisson distribution, the probability of seeing zero matches if 2.7 matches are expected is 7%. Thus, at a little less than a two-sigma confidence level, we can account for the lack of HETE/SN matches as being due to the randomness of HETE

pointing. As such, we realize that any limits from HETE will be weak.

Nevertheless, taken at face value, HETE likely *was* looking at the correct time and direction to see several SN-Ia flashes - but saw nothing. The HETE threshold is roughly 1.7×10^{-7} erg cm⁻² s⁻¹ with SN distances no farther than 43 Mpc. This forces the SN-Ia Flashes to have a luminosity of less than 4×10^{46} erg s⁻¹. With a bolometric correction, the HETE limit on the total peak luminosity will be 7×10^{46} erg s⁻¹ if the lack of matches is due to the faint luminosity of the SN-Ia Flashes.

Alternatively, we could require a covering fraction that would reduce the expected 2.7 matches down to some smaller number, but this covering fraction could be quite small and we'd still have an acceptable case with zero observed matches.

3.5.3. *Swift Limits*

Swift was watching when 16 nearby SN-Ia bursts were visible. We expect that $18\% \pm 6\%$ will have Swift covering the shock breakout. Thus, 2.9 ± 1.0 SN-Ia Flashes are expected to be detected by Swift if they were bright enough. Swift saw 0 matches, and this indicates that the SN-Ia Flashes were too faint either due to low luminosity or coverage within the progenitor system. With almost identical statistics as in the HETE case, we realize that there is a roughly two-sigma chance that the zero matches is simply due to poor luck in sky coverage.

Nevertheless, Swift was likely looking at the correct time and direction to see several SN-Ia flashes - but did not trigger on any flash. The Swift threshold is roughly 1×10^{-7} erg cm⁻² s⁻¹ with SN distances no farther than 43 Mpc. Then, the SN-Ia Flashes must have a luminosity of less than 2×10^{46} erg s⁻¹ in the 15-150 keV band. The Swift limit on the bolometric peak luminosity will be 5×10^{46} erg s⁻¹.

Again, a covering fraction could reduce the expected 2.9 matches down to some smaller number. But any limits on the covering fraction are weak.

4. Discussion

Our theoretical and observational conclusions on the peak brightness are in contradiction. That is, we predict that SN-Ia Flashes will appear as ordinary FRED GRBs with peak luminosities of $\sim 10^{48} - 10^{50}$ erg s⁻¹, however, our observational constraints show SN-Ia Flashes to have bolometric peak luminosities of less than $\sim 10^{46}$ erg s⁻¹. The observational

limits are strong since many of the known nearby SN-Ia collapses must have been observed by many GRB satellites, and so our peak luminosity limits are robust. And theoretically, there inevitably must be some sort of Flash caused both by the inevitable shock breakout and the inevitable collision of the ejecta with the accretion disk.

One possible resolution of this discrepancy is that the shock breakouts are usually covered up from Earth view, perhaps by the inner edge of an accretion disk that is much thicker than a WD radius so as to shield the WD and its shock breakout from most of the sky. Within this idea, the γ -ray flash from the ejecta ramming into the disk itself would also be absorbed by the outer parts of the disk itself. Within this idea, there would likely be two funnel regions around the poles of the accretion disk that are largely clear, such that an observer in a polar direction could still see the SN-Ia Flash. From our data, with the three satellites on patrol for ~ 15 known nearby SN-Ia events, the clear sky fraction would have to be less than 7% or so. This would give a half-opening angle of the funnel to be less than 20° or so.

Finally, we would like to point out the importance of SN-Ia Flashes (should one be detected) as diagnostical tools to constrain explosion physics and the progenitor system. There is growing evidence that mergers of pulsating delayed detonations contribute to the population of SNe Ia (Höfllich & Khokhlov 1996, Quimby et al. 2005). Even within the delayed detonation scenario and as mentioned in Section 2, the luminosity of the shock breakout depends on the chemistry of the outermost layers. In principle, observations may allow us to learn about the accretion history and possible mixing processes. Spherical symmetry implies that the nuclear outbreak occurs simultaneously. Thus, the rise to maximum light is minimized. On the other hand, recent observations of late time spectra (Höfllich et al. 2004) and early time polarization (Wang et al. 2006, Höfllich et al. 2005) suggest off-center DDTs which imply run time effects of ≈ 0.3 to 0.4 seconds. In principle, direct measurements of the rise (and the resulting change in the time evolution of the spectral energy distribution) to maximum may allow to measure these run-time effects. Finally, we have presented estimates for the burst properties but without detailed calculations. These calculations would require full 2D or 3D calculations for the interaction of the envelope with the surrounding disk, and detailed studies of the radiation processes involved. Unfortunately, the initial conditions of the disk are not well known but a knowledge is critical for detailed predictions. Alternatively, a more detailed analysis of individual events may help to constrain the properties which may include both the low and high energy photons. For the future, we plan to address gradually all these aspects.

5. Conclusions

(1) The shock breakout from the white dwarf in a Type Ia SN and the interaction of the rapidly expanding envelope with matter within the progenitor system will produce a burst of X- and γ - radiation (SN-Ia Flashes). For the shock breakout, typical peak temperatures are ~ 100 keV at peak with durations of roughly 0.1 to 0.3 seconds and peak luminosities of $\sim 10^{49} - 10^{50}$ erg s $^{-1}$. For the envelope smashing into the accretion disk, the expected durations will be roughly 1-10 seconds and the characteristic photon energies are expected to the MeV range while the peak luminosities are expected to be of order $10^{48} - 10^{50}$ erg s $^{-1}$. Both mechanisms will produce fast-rise exponential-decay shapes in their light curve. The temperature of the fireball should substantially cool over the duration of the burst.

(2) Our predicted SN-Ia Flashes events should look similar to the FRED GRBs, and might already be in the GRB catalogs. We have looked for matches between the Asiago SN catalog and the BATSE, HETE, and Swift burst lists. The BATSE constraints are the most decisive and restrictive, primarily because its sky coverage (in units of year-steradians) was a factor of ten times larger than the other two satellites. For BATSE, we have identified 33 Type Ia SNe from 19 April 1991 and 26 May 2000 whose host galaxies have radial velocities of $< 3,000$ km s $^{-1}$ (i.e., nearer than 43 Mpc for a Hubble constant of 70 km s $^{-1}$ Mpc $^{-1}$) and whose date of explosion can be determined to within 10 days. Four BATSE bursts were found to have been consistent in position (within the two-sigma BATSE circle) and time. The number of chance coincidence was determined to be 3.2 ± 0.7 , so the observed number of matches due to SN-Ia Flashes is 0.8 ± 0.7 . This non-detection of SN-Ia Flashes can be used to either limit the fraction of directions not covered (e.g. by an accretion disk) to be ≤ 12 % or to limit the average bolometric peak luminosity of $\sim 10^{46}$ erg s $^{-1}$. With the HETE and Swift satellites, we expect to see a total of 5.6 ± 1.3 SN-Ia Flashes from *known* nearby SN-Ia collapses, whereas zero were seen. This limits the peak luminosity of SN-Ia Flashes to be less than 5×10^{46} erg s $^{-1}$.

(3) The expected and observed peak luminosities are inconsistent by several orders of magnitude. The GRB satellites were watching for SN-Ia Flashes from a total of something like fifteen known events yet detected nothing, while the shock breakout and ejecta/disk interaction also are inevitable. We do not think that either the observational or theoretical results can be wrong by several orders-of-magnitude. We suggest that the initial flash of the shock breakouts and the onset of the interactions with accretion disk are hidden. Because the initial flash is not seen either, it is unlikely that material originates from a thin accretion disk or the donor star which is redistributed during hydrodynamical interactions during the explosion (e.g. Marietta et al. 2000) but it suggests a thick accretion disk or common envelope that nearly smothers the WD. We note that this result is also consistent with the

high covering factor needed to correct for the discrepancies in numbers between observed and expected supersoft X-ray sources which are regarded as possible progenitors (Rappaport et al. 1994, Kahabka & van den Heuvel 1997).

(4) Even one detection of a SN-Ia Flash will tell a substantial amount about the physics of Type Ia SNe as well as about the composition (and hence recent accretion history) of the outer layers as a guide to the progenitor type.

Finally, we also would like to stress the limits. Though multidimension effects will hardly effect the order of magnitude and the conclusions, multi-dimensional effects will become important. Secondly, the current data set is very limited and allow to estimate a covering factor of more than 88% but, to e.g. distinguish high scale heights of accretion disks from common envelopes demands a better statistics and at least one positive detection with good time and frequency coverage.

This work was supported by the grants from NSF (AST0307312 to Höflich) and from NASA (NAG5-7937 to Höflich and NNG06GH07G to Schaefer).

REFERENCES

- Barbon, R., Buond, V., Cappellaro, E., & Turatto, M. 1999, *A& AS*, 139, 531; see also <http://web.pd.astro.it/supern/snean.txt>.
- BATSE GRB Team, 2001, <http://gammaray.msfc.nasa.gov/batse/grb/catalog/current/>.
- Benz, W. Cameron, A. G. W., Press, W. H. & Bowers, R. L. 1990, *ApJ*, 348, 647
- Berger, E. et al. 2005, *Nature*, 438, 988.
- Bloom, J. S. et al. 1999, *Nature*, 401, 453.
- Bloom, J. S. et al. 2006, *ApJ*, 638, 354.
- Branch, D. 1999, *ARAA*, 36, 17
- Briggs, M. S. et al. 1999, *ApJS*, 122, 503.
- Briggs, M. S. 2001, in *Gamma-Ray Bursts in the Afterglow Era*, ed. E. Costa, F. Frontera, and J. Horth (Berlin: Springer), 22.
- Burrows, D. N. et al. 2005, *GCN Circ.* 4366.

- Campana, S. et al. 2006, *Nature*, 442, 1008.
- Cline, T. L. & Desai, U. 1974, in *Proc. 9th ESLAB Symp.* (Noordwijk: ESRO), 37.
- Cline, T. L. et al. 1980, *ApJ*, 237, L1.
- Colgate, S. A. 1968, *Canadian J. Phys.*, 46, S476.
- Colgate, S. A. 1970, *Acta Physica Academiae Scientiarum Hungaricae*, 29, Suppl. 1, pp. 353-359.
- Colgate, S. A. 1974, *ApJ*, 187, 333.
- Dado, S. & Dar, A. 2005, *GCN Circ.* 3423.
- Dar, A. 1999, *A&AS*, 138, 505.
- Dar, A. & De Rujula, A. 2004, *Physics Reports*, 405, 203.
- Della Valle, M. et al. 1993, *IAUCirc.* 5782.
- Deng, M. 2001, Ph. D. Thesis, Yale University.
- Evans, W. D. et al. 1980, *ApJ*, 237, L7.
- Felten, J. E. 1982, 17th International Cosmic Ray Conference, Paris, 9, 52-55.
- Fenimore, E. E. & Ramirez-Ruiz, E. 2000, *astro-ph/0004176*.
- Filippenko, A. V. & De Breuck, C. 1998, *IAUCirc.* 6997.
- Filippenko, A. V. et al. 1992, *AJ*, 104, 1543.
- Fisher A., Branch D., Hatano K., Baron E. 1999, *MNRAS*, 304, 679
- Fishman, G. J. et al. 1994, *ApJSupp*, 92, 229.
- Ford, C. H. et al. 1993, *AJ*, 106, 1101.
- Fox, D. B. et al. 2005, *Nature*, 437, 845.
- Galama, T. J. et al. 1998, *Nature*, 395, 670.
- Galama, T. J. et al. 2000, *ApJ*, 536, 185.
- Garnavich, P. 1996, *IAUCirc.* 6503.

- Gehrels, N. et al. 2004, ApJ, 611, 1005.
- Gehrels, N. et al. 2005, Nature, 437, 851.
- Gerardy, C. L., Höflich, P., Fesen, R. A., Marion, G. H., Nomoto, K., Quimby, R., Schaefer, B. E., Wang, L., & Wheeler, J. C. 2004, ApJ, 607, 1258
- Hatano, K., Branch, D., Fisher, A., Baron, E., & Filippenko, A. V. 1999, ApJ, 525, 881
- Hatano K., Branch D., Lentz E. J., Baron E., Filippenko A. V., Garnavich P. 2000, ApJ 543L, 49
- Heise, J., in't Zand, J., Kippen, R. M., & Woods, P. M. 2001, in Gamma-Ray Bursts in the Afterglow Era, ed. E. Costa, F. Frontera, and J. Horth (Berlin: Springer), 16.
- Hjorth, J. et al. 2003, Nature, 423, 847.
- Hjorth, J. et al. 2005, Nature, 437, 859.
- Ho, W. C. G. et al. 2001, PASP, 113, 1349.
- Höflich P. 2005, Nuclear Physics A, 777, 579
- Höflich P., Gerardy C., Quimby R., 2005, New Astronomy, 50, 470
- Höflich, P., Gerardy C., Nomoto K., Motohara K., Fesen R.A., Maeda K., Ohkubo T., Tominaga N, ApJ, 617, 1258
- Höflich, P., Gerardy, C., Linder, E., & Marion, H. 2003, Lecture Notes in Physics 635, Springer Press, p. 203 & astro-ph/0301334
- Höflich, P., Gerardy, C., Fesen, R., & Sakai, S. 2002, ApJ, 568, 791
- Höflich P., 2002b, in: Theory of Stellar Atmospheres, eds. I. Hubeney, D. Mihalas & C. Werner, ASP Conference Series, Vol. 288, p. 371
- Höflich P., 2002b, in: Theory of Stellar Atmospheres, eds. I. Hubeney, D. Mihalas & C. Werner, ASP Conference Series, Vol. 288, p. 185
- Höflich, P., Gerardy, C., Fesen, R. A., & Sakai, S. 2002, ApJ, 568, 791.
- Höflich P., Khokhlov A. 1996, ApJ, 457, 500
- Höflich P., Wheeler J. C., Thielemann F. K. 1998, ApJ, 495, 617

- Höflich P. 1995, ApJ, 443, 89
- Höflich P., Khokhlov A., Müller E. 1993, A&A, 270, 223
- Hurley, K. 2000, in Gamma-Ray Bursts: 5th Huntsville Symposium, ed. R. M. Kippen, R. S. Mallozzi, and G. J. Fishman (Melville NY, AIP Conf. Proc. 526), 763.
- Hurley, K. et al. 1999, ApJSupp, 120, 399.
- Hurley, K. et al. 2000, ApJ, 534, 258; see also <http://ssl.berkeley.edu/ipn3/index.html>.
- Hurley, K. et al. 2005, Nature, 434, 1098.
- Jha, S., Challis, P., & Kirshner, R. 2000, IAUCirc. 7437.
- Kahabka, P., van den Heuvel, E.P.J. 1997, A&A 35, 69
- Kippen, R. M. et al. 1998, ApJ, 506, L27.
- Kippen, R. M., Woods, P. M., Heise, J., in't Zand, J., Preece, R. D., & Khokhlov A. 1991, ApJ, 245, 114
- Kirshner, R. P. 1993, ApJ, 415, 589.
- Klebesadel, R. W., Strong, I. B., & Olson, R. A. 1973, ApJ, 182, L85.
- Kouveliotou, C. et al. 1993, ApJ, 413, L101.
- Kouveliotou, C. et al. 1993, ApJ, 567, 447.
- Krisciunas, K. et al. 2000, ApJ, 539, 658.
- Kulkarni, S. et al. 1998, Nature, 395, 663.
- Leibundgut, B. et al. 1993, AJ, 105, 301.
- Li, W. D. et al. 1999, AJ, 117, 2709.
- Li, W. D. et al. 2003, PASP, 115, 453.
- Lira, P. et al. 1998, AJ, 115, 234.
- MacFadyen, A. I., Woosley, S. E., & Heger, A. 2001, ApJ, 550, 410.
- Malesani, D. et al. 2004, ApJLett, 609, L5.

- Marion, G. H., Höflich, P., Vacca, W. D., & Wheeler, J. C. 2003, *ApJ*, 591, 316
- Maza, J. 1998, *IAUCirc.* 6978.
- Marietta E., Burrows A., Fryxell B. 2000, *ApJ.Suppl.* 128, 615
- Mattila et al. 2005, *A&A*, 443, 649
- McNaught, R. N., Della Valle, M., & Leisy, P. 1991, *IAUCirc.* 5258.
- Modjaz, M. et al. 1998, *IAUCirc.* 6993.
- Nakano, S. et al. 1999, *IAUCirc.* 7328.
- Nomoto, K., Uenishi, T., Kobayashi, C., Umeda, H., Ohkubo, T., Hachisu, I., & Kato, M. 2003, in: *From Twilight to Highlight: The Physics of Supernovae*, eds. W. Hillebrandt & B. Leibundgut, *ESO Astrophysics Symposia* (Berlin:Springer), 115 (astro-ph/0308138)
- Norris, J. P., Marani, G., & Bonnell, J. 2000, *ApJ*, 534, 248.
- Paciesas, W. C. et al. 1999, *ApJSupp*, 122, 465.
- Pain, R. et al. 1996, *ApJ*, 473, 356.
- Patat, F. & Maia, M. 1998, *IAUCirc.* 6888.
- Phillips, M. M., Kunkel, W., & Filippenko, A. V. 1999, *IAUCirc.* 7122.
- Pozdnyakov L.A., Sobol I.M., Syunyaev R.A., 1976, *Soviet Astr. Let.* 2, 55
- Quimby R., Höflich P., Kannapa S.J., Rykoff E., Rujopakarn W., Akerlof C.W., Gerardy C., Wheeler J.C. 2005, *ApJ*, in press
- Qiao, Q. Y., Qiu, Y. L., Li, W. D., & Hu, J. Y. 1999, *IAUCirc.* 6775.
- Rappaport S/., Chiang, E., Kallman, T., Malina, R. 1994, *ApJ* 431, 237
- Reichart, D. E. 1999, *ApJ*, 521, L111.
- Riess, A. G., Nugent, P., Filippenko, A. V., Kirshner, R. P., &
- Paczynski B., 1985, in: *Cataclysmic Variables and Low-Mass X-Ray Binaries*, eds. D.Q. Lamb, J. Patterson, Reidel, Dordrecht, p.1
- Perlmutter, S. 1998, *ApJ*, 504, 935.

- Riess, A. G., Press, W. H., & Kirshner, R. P. 1996, *ApJ*, 473, 88.
- Riess, A. G. et al. 1999a, *AJ*, 117, 707.
- Riess, A. G. et al. 1999b, *ApJ*, 118, 2675.
- Sadakane, K. et al. 1996, *PASJ*, 48, 51.
- Salvo, M. E. et al. 2001, *MNRAS*, 321, 254.
- Schaefer, B. E. 1996, *ApJ*, 464, 404.
- Schaefer, B. E. 2006, *ApJLett*, 642, L25.
- Schaefer, B. E. & Deng, M. 2000, in *Gamma-Ray Bursts: 5th Huntsville Symposium*, ed. R. M. Kippen, R. S. Mallozzi, and G. J. Fishman (Melville NY, AIP Conf. Proc. 526), pp. 419-423. Schaefer, B. E. 2003, *ApJ*, 583, L71.
- Schaefer, B. E. et al. 2003, *ApJ*, 588, 387.
- Schmidt, B. 1998, *IAUCirc.* 6989.
- Soderberg, A. M. et al. 2006, *ApJ*, 650, 261.
- Stanek, K. Z. et al. 2003, *ApJ*, 591, L17.
- Taylor, J.H 1994, *Rev. Mod. Phys.* 66, 711
- Terlevich, R. & Fabian A. 1999, *IAUCirc.* 7269.
- Toth, I. & Szabo, R. 2000, *A&A*, 361, 63.
- Turatto, M., Pastorello, A., Cappellaro, E., & Cedrati, F. 2000, *IAUCirc.* 7438.
- Turatto, M. et al. 1996, *MNRAS*, 283, 1.
- Vacca, W. D. & Leibundgut, B. 1996, *ApJ*, 471, L37.
- Van den Heuvel, E.P.J., Bhattacharya, D., Nomoto, K., Rappaport, S. 1992, *A&A* 262, 97
- Villasenor, J. S. et al. 2005, *Nature*, 437, 855.
- Vink, J. et al. 2001, *A&A*, 372, 824.
- van den Bergh, S. & Tammann, G. A. 1991, *ARA&A*, 29, 363.
- Waxman E.; Meszaros P., Campana S. 2007, *ApJ*, accepted, & arXiv:astro-ph/0702450

Wang, L. & Wheeler, J. C. 1998, ApJ, 504, L87.

Wang, L., Baade, D., Höflich, P., Khokhlov, A, Wheeler, J. C., Kasen, D., Nugent P.,
Perlmutter S., Fransson C., Lundqvist P. 2003, ApJ 591, 1110

Wang, L., Baade, D., Höflich, P., Wheeler J.C., Kawabata, K., Khokhlov, A, Nomoto, K.,
Patat, F.2006 ApJ, 653, 490

Webbink R. F. 1984, ApJ, 277, 355

Whelan J., Iben Jr. I. 1973, ApJ, 186, 1007

Woosley, S. E. & Bloom, J. S. 2006, ARA&A, 44, 507.

Table 1. SN-Ia Matches with BATSE GRBs

SN	RV (km/s)	Ref. ^a	T_{peak}	T_{exp}	GRB	Θ/σ_{BATSE}	ΔT (days)
1991 T	1732	1	Apr 28.7±2(B)	Apr 8±3
1991 X	2626	2	May 5±7	Apr 15±8	910423	0.57	8±8
1991 bg	913	3-5	Dec 13±2(B)	Nov 29±5	911125	0.6	4±5
1992 A	1845	6	Jan 19.2±2(B)	Jan 1±3
1992 G	1580	7	Feb 21.1±2(V)	Feb 1±5
1993 L	1925	8	Apr 19±10	Apr 3±10
1994 D	450	9	Mar 20.9±2 (B)	Mar 5±3
1994 U	1329	10	Jul 5±7	Jun 15±8	940621	2.21	6±8
1994 ae	1282	11, 12	Nov 30±2	Nov 10±5
1995 D	1967	11-13	Feb 21.5±2	Feb 1±5
1995 al	1541	14	Nov 7.1±2(B)	Oct 15±3
1996 X	2032	14, 15	Apr 18±2(B)	Mar 31±3
1996 Z	2275	14	May 13±2(B)	Apr 25±3
1996 ai	992	14	Jun 20.8±2(B)	May 31±3
1996 bk	2041	14	Oct 9.0±5(B)	Sep 25±7	960916	2.81	9±7
1996 bt	2675	16	Nov 1±7	Oct 11±8	961017	2.89	6±8
1997 bp	2492	10	Apr 7±7	Mar 18±8
1997 bq	2813	17	Apr 17±2	Mar 30±3	970331	1.29	1±3
1997 br	2069	18	Apr 20.3±2	Mar 30±3
1997 dt	2191	19	Nov 22±7	Nov 2±8
1998 aq	924	17	Apr 27±2	Apr 8±3	980406	1.04	2±3
1998 bn	1828	20	Apr 30±5	Apr 10±7
1998 bu	943	17	Apr 18±2	Mar 30±3
1998 dg	2454	21, 22	Jul 30±10	Jul 10±10
1998 dh	2669	17	Aug 2±2	Jul 15±3	980712	2.88	3±3
1998 dm	1943	23, 24	Aug 28±5	Aug 13±7
1999 ac	2848	25	Mar 1±5	Feb 7±7	990206	2.62	1±7
1999 by	638	26, 27	May 11.25±2	Apr 27±5
1999 cl	2120	28	Jun 15±2	May 26±5
1999 cp	2823	28	Jun 18±5	May 29±7
1999 gh	2310	29	Dec 3±7	Nov 13±8
2000 E	1331	30	Feb 3±2	Jan 14±3
2000 cm	2170	31, 32	May 22±10	May 2±10	000508	2.52	6±10

^aReferences. — 1. Lira et al. 1998. 2. McNaught, Della Valle, & Leisy 1991. 3. Leibundgut et al. 1993. 4. Filippenko et al. 1992. 5. Turatto et al. 1996. 6. Kirshner et al. 1993. 7. Ford et al. 1993. 8. Della Valle et al. 1993. 9. Vacca & Leibundgut 1996. 10. Riess et al. 1998. 11. Ho et al. 2001. 12. Riess, Press, & Kirshner 1996. 13. Sadakane et al. 1996. 14. Riess et al. 1999a. 15. Salvo et al. 2001. 16. Garnavich 1996. 17. Riess et al. 1999b. 18. Li et al. 1999. 19. Qiao et al. 1999. 20. Patat & Maia 1998. 21. Maza 1998. 22. Schmidt 1998. 23. Modjaz et al. 1998. 24. Filippenko & De Breuck 1998. 25. Phillips, Kunkel, & Filippenko 1999. 26. Höflich et al. 2002. 27. Toth & Szabo 2000. 28. Krisciunas et al. 2000. 29. Nakano et al. 1999. 30. Vinkó et al. 2001. 31. Jha, Challis, & Kirshner 2000. 32. Turatto et al. 2000.

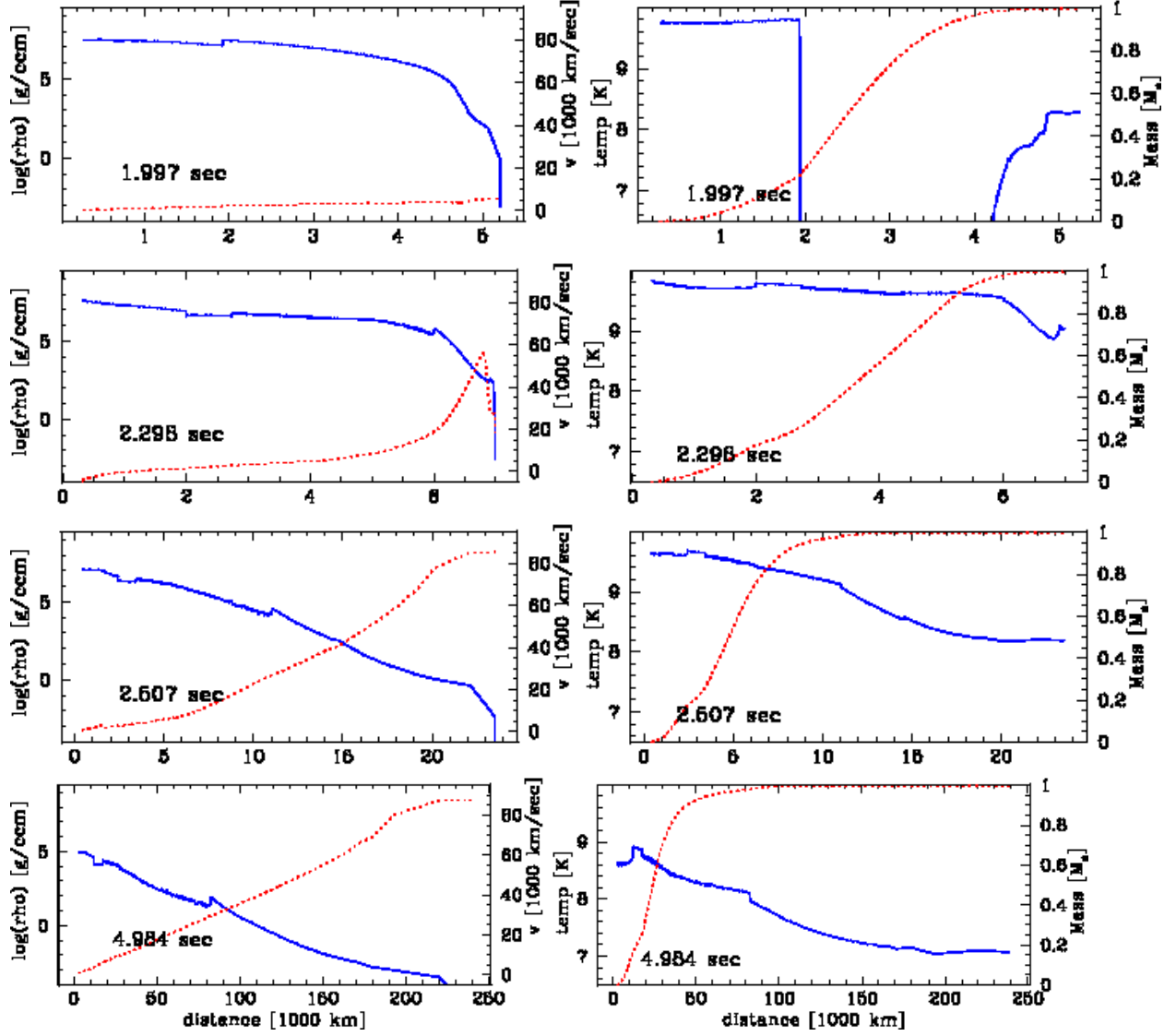


Fig. 1.— Structure of the delayed detonation model as a function of distance at various stages of the explosion, namely a) during the deflagration phase, b) at the shock breakout, c) during the strong acceleration phase of the outer layers, and d) close to homologous expansion. We give the density (solid, left scale), velocity (dotted, right scale), and the logarithm of the temperature (solid, left scale), enclosed mass (dotted, right scale), respectively.

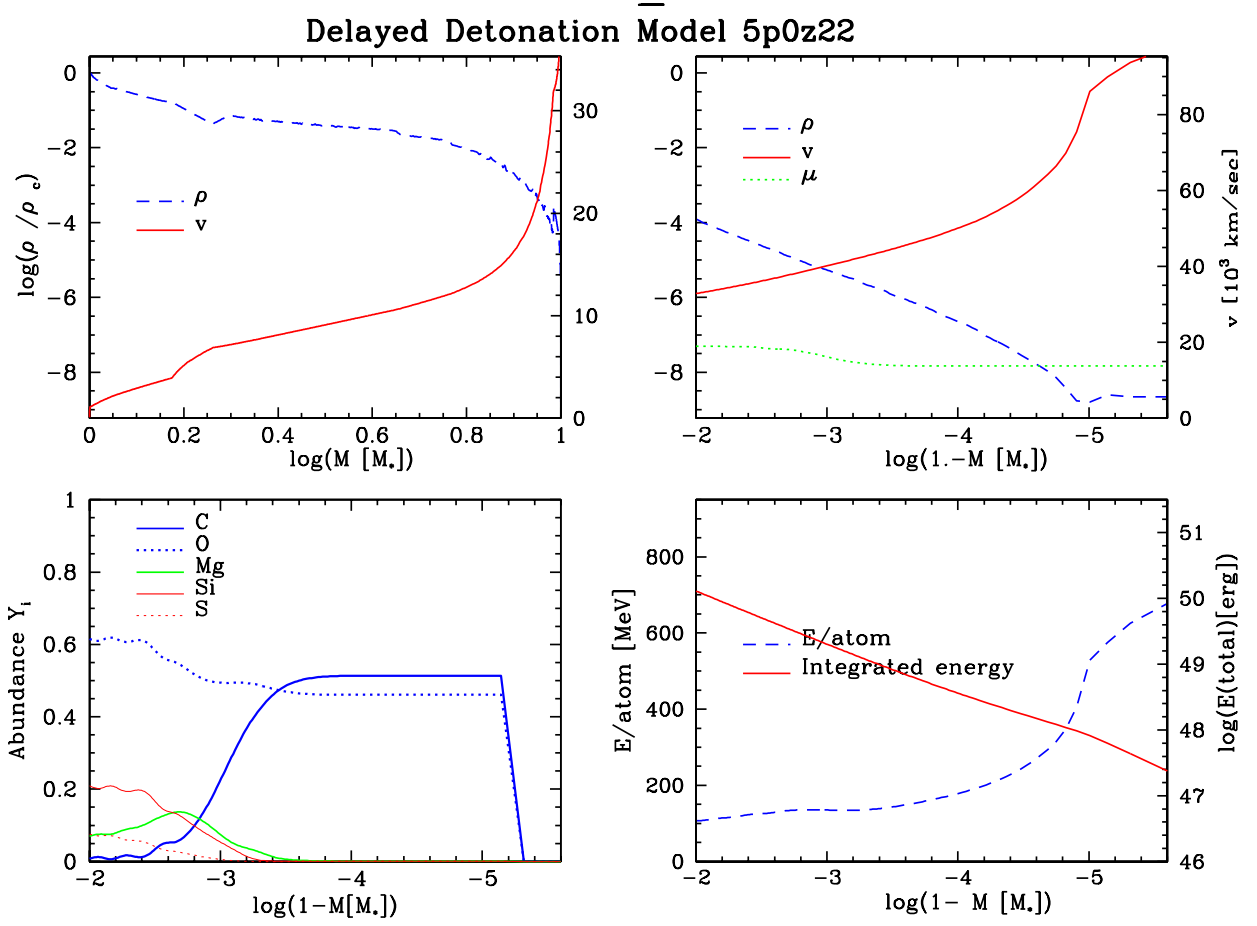


Fig. 2.— The density, velocity, and mean molecular weight at about 10 seconds after the explosion (upper plots) are given with the scale on the left and right, respectively. At this time, the expansion is close to homologous. On the lower left, the chemical abundances for the outer $10^{-2}M_\odot$. For the full profiles, see Höflich et al. (2002). Outside $5 \times 10^{-6}M_\odot$ the abundance is solar. In addition, the mean energy per atom (right scale) and the integrated kinetic energy (from the surface) are given on the lower right.

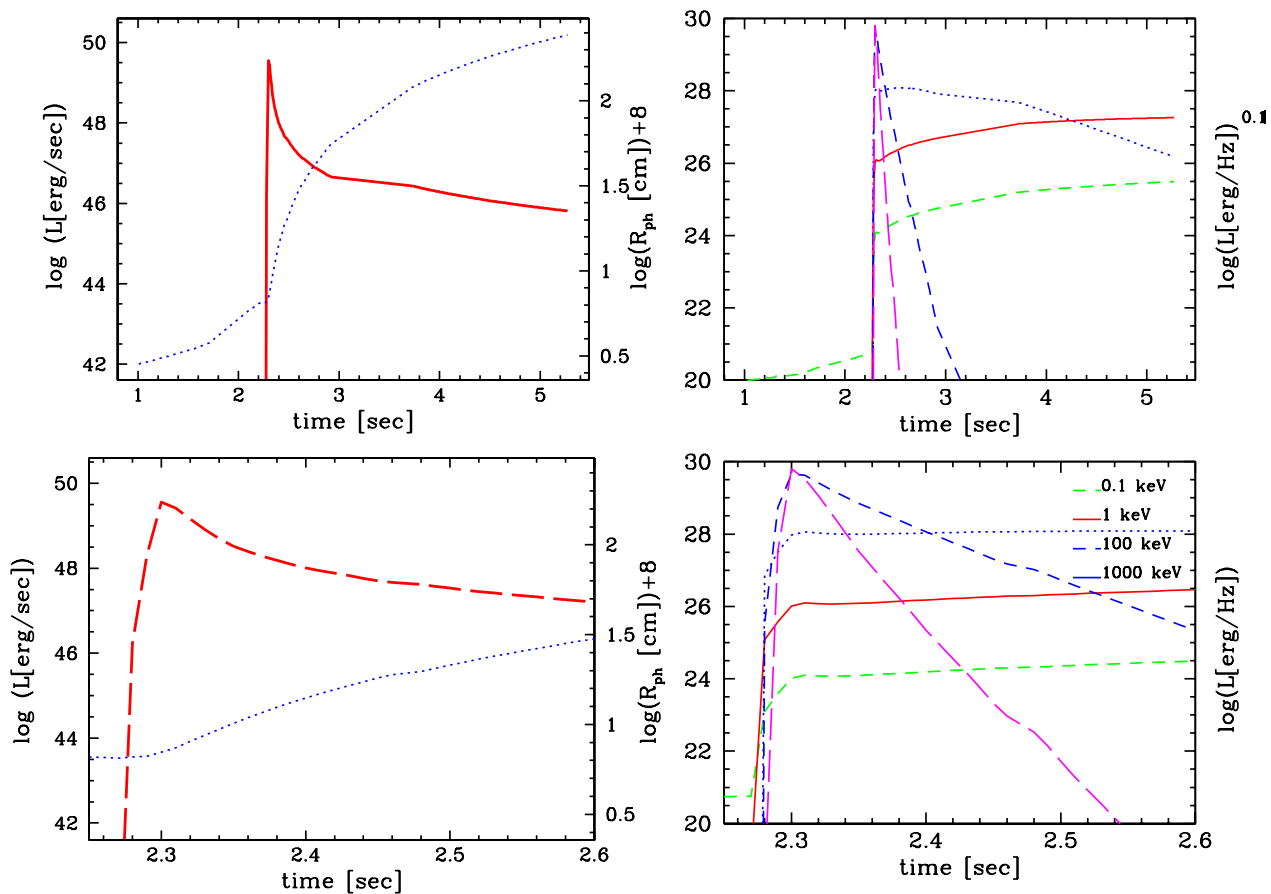


Fig. 3.— Bolometric and monochromatic luminosities as a function of time. In addition, the evolution of the photospheric radius is given which is within the outer $10^{-4}M_{\odot}$ during at the first minute.